

# Synthesis and Characterization of a Novel Proton-Exchange Membrane for Fuel Cells Operating at High Temperatures and Low Humidities

Ching-Nan Chuang,<sup>1,2</sup> Liang Chao,<sup>3</sup> Ying-Jie Huang,<sup>4</sup> Tar-Hwa Hsieh,<sup>1,2</sup> Hung-Yi Chuang,<sup>1,2</sup> Shu-Chi Lin,<sup>1,5</sup> Ko-Shan Ho<sup>1</sup>

<sup>1</sup>Department of Chemical and Material Engineering, National Kaohsiung University of Applied Sciences, 415 Chien-Kuo Road, Kaohsiung 807, Taiwan

<sup>2</sup>Institute of Polymer Science and Engineering, National Taiwan University, Section 1, 4 Roosevelt Road, Taipei, Taiwan

<sup>3</sup>Center for General Education, Technology and Science Institute of Northern Taiwan, Peito, Taipei 11202, Taiwan

<sup>4</sup>Institute of Nanotechnology, National Chiao Tung University, 1001 Ta Hsueh Road, Hsinchu, Taiwan

<sup>5</sup>Group of Bio-Instructor, Madou Junior High School, 36 Nan-Shi District, Madou, Tainan County 721, Taiwan

Received 11 April 2007; accepted 18 September 2007

DOI 10.1002/app.27437

Published online 10 December 2007 in Wiley InterScience (www.interscience.wiley.com).

**ABSTRACT:** The synthesis of a *p*-toluidine/formaldehyde (PTF) resin was performed, and the effects of the molar ratio of the individual monomers and the polymerization conditions on the structure of the PTF resin were studied. Fourier transform infrared and <sup>13</sup>C-NMR spectra were used to characterize the PTF. Wide-angle X-ray diffraction patterns revealed the crystalline structures of various PTFs. Polarized optical microscopy revealed that the molar ratio of the monomers had a strong effect on the crystalline morphologies. A longer polymerization time turned out a polymer with a higher intrinsic viscosity and molecular weight, which led to differences in the proton

conductivity. All of the PTFs showed a higher proton conductivity than a commercial Nafion membrane at 90–100°C and 0% relative humidity. The proton conductivity of the PTF series could be improved by sulfonation with sulfuric acid and could be maintained after blending with polyurethane. Pure methanol could be used as a fuel source because of the insolubility and nonwetting properties of PTF in methanol to increase the output current density for a PTF membrane electrode assembly. © 2007 Wiley Periodicals, Inc. *J Appl Polym Sci* 107: 3917–3924, 2008

**Key words:** membranes; resins; solid state structure

## INTRODUCTION

Fuel-cell technology has been considered a promising alternative for supplying clean and highly efficient power instead of the burning of fossil oil.<sup>1–3</sup> There are several kinds of fuel cells available: alkaline fuel cells, phosphoric acid fuel cells, solid oxide fuel cells, molten carbonate fuel cells, proton-exchange membrane fuel cells, and direct methanol fuel cells. Among these types of fuel cells, proton-exchange membrane fuel cells and direct methanol fuel cells are known to perform by the use of proton-exchange membranes (PEMs) as solid-state electrolytes for the conveyance of protons between electrodes. The most commonly used and commercially available PEMs are based on a perfluorinated ionomer, such as Nafion from Dupont; a partially

fluorinated polymer, such as poly(vinylene fluoride-grafted-sulfonated polystyrene (PVDF-*g*-SPS);<sup>4</sup> a hydrocarbon polymer, such as sulfonated poly(ether ether ketone),<sup>5–7</sup> poly(phenylene oxide),<sup>8,9</sup> or polybenzimidazole;<sup>10–13</sup> and a block copolymer, such as sulfonated poly(styrene isobutylene styrene).<sup>14</sup> Polymers based on solid-state electrolytes can be used in lots of high-technical areas and have attracted much attention in past decades. Most studies have focused on the design of novel polymer materials possessing high ionic conductivities and better mechanical properties, durability, and chemical and thermal resistance for industrial purposes.<sup>15–17</sup> For a regular PEM, proton movement comes from the help of the abundant water molecules absorbed around the PEM, and this means that the membrane should absorb as much water as it can to maintain the high ionic conductivity. However, water evaporates easily because of the heat that evolves from the performance of the fuel cells, which can largely slow down the movement of the protons and the ionic conductivity. In other words, the lifetime of this kind of fuel cell will be shortened unless it can preserve its high humidity during or after performance from

Correspondence to: K.-S. Ho (hks@cc.kuas.edu.tw).

Contract grant sponsor: National Science Council (Taiwan, Republic of China); contract grant numbers: 95-2221-E-151-055 and 95-2622-E-151-025-CC3.

*Journal of Applied Polymer Science*, Vol. 107, 3917–3924 (2008)  
© 2007 Wiley Periodicals, Inc.

the aqueous fuel, which needs a good fuel-barrier membrane and a high-water, low-fuel-concentration fuel source, which results in a limited output current or voltage of the fuel cell.

Therefore, we refer to the performance of a dry, solid-state membrane used in lithium batteries. Most of these membranes are made of poly(ethylene oxide) (PEO) derivatives that can convey lithium ions through coordinate bonding under totally dry conditions. The studies on PEO started with the work of Wright and coworkers<sup>18,19</sup> in 1975. They found that PEO complexed with alkali metal salts (e.g., KSCN) could exhibit high ionic conductivity even at elevated temperatures. Armand et al.<sup>20(a)</sup> recognized the potential applications of these polymer electrolytes as separators in solid-state batteries and then found that ions are actually transported within the helical channels of PEO molecules. Hardy and Shriver<sup>20(b)</sup> reported that ions could move faster in an amorphous polymer electrolyte with a low glass-transition temperature ( $T_g$ ). A complexation similar to the coordination bonding between lithium ions and the etheryl groups of PEO can occur between the protons and amino groups of a *p*-toluidine/formaldehyde (PTF) resin, whose crystallinity and molecular weight (related to  $T_g$ ) can be altered by changes in the reaction (polymerization) conditions, such as the reactant ratio and time. In this study, a PEM with good proton conductivity at high temperatures [from room temperature (RT) to 100°C] under low-humidity conditions was prepared.

## EXPERIMENTAL

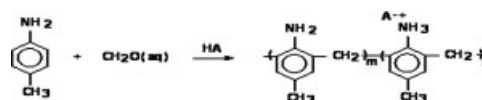
### Materials and reagents

The *p*-toluidine crystals were purchased from Acros (Taiwan) without any further purification. The other chemicals were all obtained from Aldrich and used as received, including formaldehyde (37.2 wt % aqueous solution), concentrated sulfuric acid (98%), methanol, and toluene.

### Synthesis and sample preparation

Preparation of the PTF resin with different reaction times

Similarly to the preparation of novolac-type phenol formaldehyde through condensation polymerization,<sup>21</sup> the PTF resin was obtained by the polymerization of *p*-toluidine with an equivalent amount of formaldehyde in the presence of acids, as illustrated in Scheme 1. *p*-Toluidine (21.4 g, 0.2 mol) was added to a 500-mL, four-necked flask fitted with a reflux condenser and a mechanical stirrer. After the reactant was heated to 120°C in the reactor, 2 g of con-



Scheme 1 Synthesis of the PTF resin.

centrated sulfuric acid was slowly added, and a 37.2% solution of formaldehyde (12.6 mL, 0.16 mol) was added dropwise within 60 min. The reaction lasted 6 and 24 h, respectively, before the flask was opened and an additional 2 g of concentrated sulfuric acid was introduced to absorb (remove) the excess or condensed water. The obtained PTF resin was immersed in toluene and filtered to remove residual *p*-toluidine. The cake was dried in a vacuum oven at 60°C for 24 h. The dried sample was characterized with Fourier transform infrared (FTIR) and NMR spectrometry, respectively.

Preparation of the PTF resin with different molar ratios

Formaldehyde (37.2% aqueous solution) and *p*-toluidine (analytical grade) in various molar ratios (0.8/1, 1/1, and 1.2/1) were mixed together in the presence of acids in a 500-mL, four-necked flask fitted with a reflux condenser and a mechanical stirrer. The mixture was heated to 120°C and stayed there for 24 h. The mixture was then cooled to RT and put into a toluene pool to remove residual *p*-toluidine; this was followed by filtration and drying *in vacuo* at 60°C for 24 h. The dried sample was characterized with FTIR and <sup>13</sup>C-NMR spectra.

Preparation of polyurethane (PU) and its blend with the PTF resin

PU in an *N*-methylpyrrolidone (NMP) solution was prepared through the mixing of equal moles of polytetramethylene oxide (PTMO) 650 with MDI in NMP. The obtained NMP solution of PU was put into different proportions of PTF and stirred overnight. The blend solution was cast onto a Petri dish before being dried in a vacuum oven at 50°C for at least 48 h to obtain a PTF/PU polyblending film.

### Measurements

FTIR spectrometry

The FTIR spectra of various samples were obtained with a PerkinElmer 69002 FTIR instrument with a resolution of 4 cm<sup>-1</sup> and 16 scans in dry KBr. The scan was performed from 4000 to 400 cm<sup>-1</sup>.

### <sup>13</sup>C-NMR spectroscopy

For characterization by <sup>13</sup>C-NMR spectra, different PTFs prepared under different polymerization conditions were first dissolved in the solvent deuterated dimethyl sulfoxide and subjected to the regular measuring procedures of a Varian Unity Plus NMR spectrometer, which was operated at 400 MHz. The <sup>13</sup>C chemical shifts were externally referenced to tetramethylsilane.

### Wide-angle X-ray diffraction (WAXD)

A Rigaku D-2000 X-ray generator (Japan) with a Cu K $\alpha$  target ( $\lambda = 1.5406 \text{ \AA}$ ) was used to obtain X-ray diffraction patterns at 2°/min. The scattering angle ( $2\theta$ ) ranged from 2 to 40°.

### Polarized optical microscopy (POM)

The samples were first dissolved in methanol and onto a microscope glass plate ( $7.6 \times 2.54 \times 0.1 \text{ cm}$ ) to evaporate methanol and then were dried in a vacuum oven at 60°C for 24 h. An Olympus model BH-2 polarized optical microscope (Japan) was used to take pictures of PTF resins with different reaction ratios at a magnification of 200 $\times$ .

### Intrinsic viscosity

The PTF resin with different polymerization times was dissolved in concentrated sulfuric acid (0.6 g/dL) at 30°C, and the intrinsic viscosity was measured with a Cannon-Fenske viscometer according to eq. (1):

$$[\eta] = \frac{1}{C} \sqrt{2(\eta_{sp} - \ln \eta_r)} \quad (1)$$

where  $[\eta]$  is the intrinsic viscosity,  $\eta_{sp}$  is the specific viscosity, and  $\eta_r$  is the relative viscosity.

### Electrochemical impedance spectroscopy

The proton conductivity was measured with an electrochemical alternating-current impedance spectroscopy technique over the frequency range of 100 Hz to 100 MHz. The resistance of PTF was measured with an Autolab PGSTAT 30 impedance analyzer (The Netherlands). The proton conductivity was determined with eq. (2):

$$\sigma(\text{S/cm}) = \frac{d}{Z'_0 \times A} \quad (2)$$

where  $\sigma$  is the conductivity,  $Z'_0$  is the extrapolated real-part of the impedance when the imaginary im-

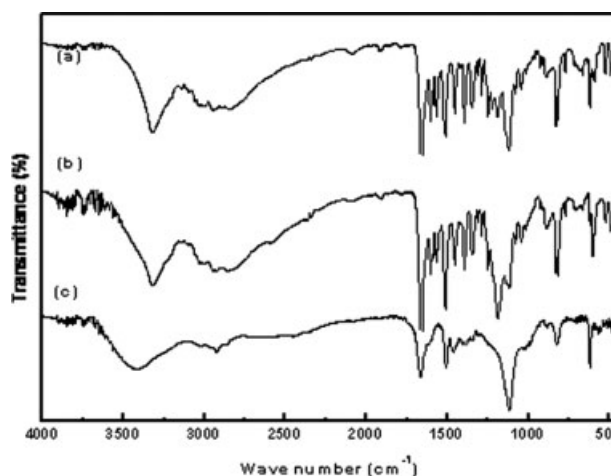
pedance is zero (the intercept crosses the  $Z'$  axis),  $A$  is the cross-sectional area, and  $d$  is the thickness of the PTF sample.

## RESULTS AND DISCUSSION

### Characterization

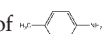
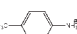
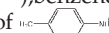
The characteristic absorption peaks of the PTF resin with different molar ratios are shown in Figure 1. Figure 1 reveals the presence of stretching at 3326  $\text{cm}^{-1}$ , which belongs to the amine group of polymerized *p*-toluidine of PTF. Also, there are characteristic absorption peaks at 1120  $\text{cm}^{-1}$  for ether groups and at 601 and 1191  $\text{cm}^{-1}$  corresponding to the asymmetric and symmetric stretching of complexed sulfonic groups. Except for the ortho-ortho linking (830  $\text{cm}^{-1}$ ), the *para*-methyl groups of *p*-toluidine can be found at 820  $\text{cm}^{-1}$  from the spectral analysis. Only Figure 1(c) demonstrates 3422  $\text{cm}^{-1}$  due to the presence of the stretching —OH group obtained from excess formaldehyde, which can form the etheryl backbone and hydroxyl chain ends and accounts for the better water solubility.<sup>22</sup> These hydroxyl chain ends allow us to perform any modification of the PTF membrane, such as changes in the methanol-barrier property and the attachment of hydrophobic groups. The assignments of the infrared spectrum are listed in Table I.

The <sup>13</sup>C-NMR spectra were used to characterize PTF prepared with different polymerization times and various monomer ratios. Figure 2(a) reveals the resonance peaks of PTF with less and equal molar amounts of formaldehyde. The corresponding carbons are numbered with the attached chemical structure. The aromatic carbons of PTF can be seen around 110–150 ppm (nos. 1–8). The methylene car-



**Figure 1** FTIR spectra of the PTF resin with different molar ratios of formaldehyde to *p*-toluidine: (a) 1/0.8, (b) 1/1, and (c) 1.2/1.

**TABLE I**  
Assignments of the Infrared Spectrum of PTF

Frequency (cm <sup>-1</sup> )	Assignment
3422	v(-OH)
3500-3200	v(-NH of  , or  )
2960-2850	v <sub>as</sub> and v <sub>sy</sub> (-CH <sub>3</sub> )
2920	v(-CH <sub>2</sub> -)
1600	v(-C=C-), benzene ring
1600-1575	δ(-NH of  )
1450	δ(-CH <sub>2</sub> -)
1370-1250	v(-C-N-)
1120	v(-O-)
1191	δ(-O=S=O) of -SO <sub>3</sub> -
620	δ(-S=O) of -SO <sub>3</sub> -
830	( <i>o,o'</i> , <i>p</i> )-Substitution
820	<i>p</i> - and ( <i>o,p</i> )-substitution
773	<i>o</i> -Substitution

bonds of PTF, which link benzene rings together, are significantly demonstrated around 38–42 ppm (nos. 10 and 11). The para-substituting methyl to the aromatic ring is approximately located at 20 ppm (no. 9). The spectrum of PTF with excess formaldehyde, which is illustrated in Figure 2(b) (which shows the molar ratio of formaldehyde to *p*-toluidine), reveals

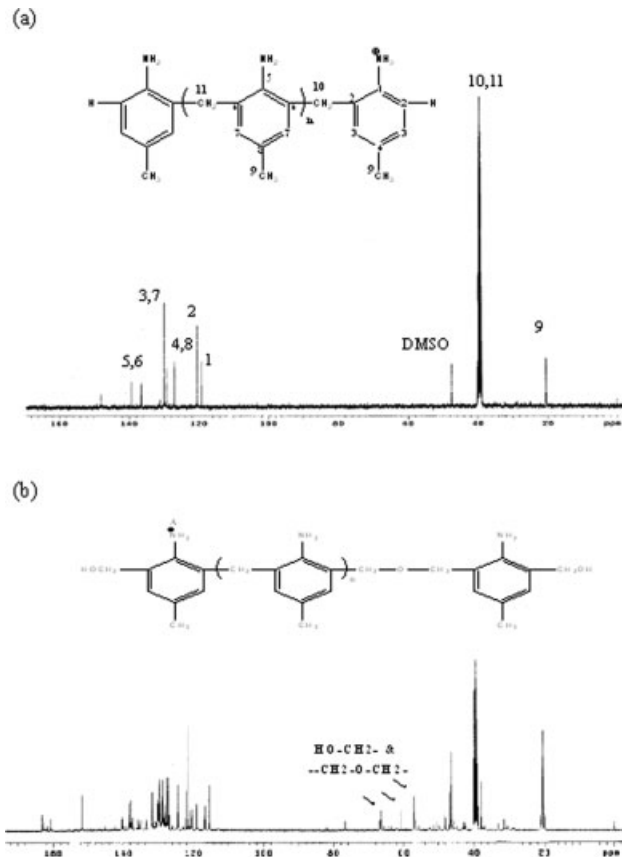


**Figure 2** <sup>13</sup>C-NMR spectra of PTF with different molar ratios of formaldehyde to *p*-toluidine: (a) 1/0.8 or 1/1 and (b) 1.2/1.

extra resonance peaks around 50 ppm for hydroxyl and etheryl methylenes and wide-ranging aromatic carbon resonance peaks around 110–170 ppm. The additional resonance peak comes from the etheryl linkages derived from the excess formaldehyde, where hydroxyl chain ends can condense into ether. In other words, they can terminate the PTF molecules with methanol groups, and this makes its NMR spectrum more complicated. The presence of several peaks in this region indicates that there are hydrogen-bonded and non-hydrogen-bonded methanol chain ends present.

### WAXD patterns

If aniline is used for polymerization with formaldehyde, it will produce a resin without any crystallinity because of the presence of the ortho-para polymerization, except for the ortho-ortho polymerization of aniline monomers.<sup>22-24</sup> However, crystallinity can be found if aniline is replaced by *p*-toluidine, for which only ortho-ortho polymerization is possible. The WAXD patterns of PTF resins of different monomer ratios are shown in Figure 3. In Figure 3, different molar ratios show different crystalline pattern peaks. The polymerization with a formaldehyde/*p*-toluidine molar ratio of 0.8/1 exhibits a characteristic peak at  $2\theta = 5.65^\circ$ , which is the PTF resin layer-to-layer distance. When the molar ratio is 1, a new characteristic peak is revealed with  $2\theta = 4.75^\circ$ . Excess formaldehyde [Fig. 3(c); formaldehyde/*p*-toluidine = 1.2/1] shows an insignificant peak in a low-angle region due to the presence of the softer etheryl groups of the backbone, which make it more difficult to maintain a well-defined crystalline structure. However, the methanol terminal chain ends can create strong hydrogen bonds between the molecules, destroy the original crystalline structure,

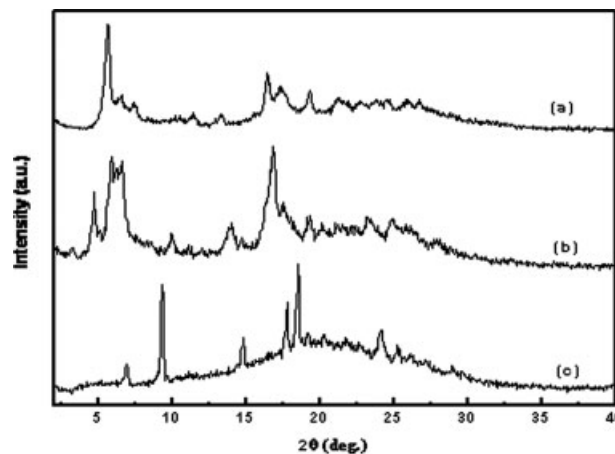


**Figure 3** X-ray diffraction patterns of the PTF resin with different molar ratios of formaldehyde to *p*-toluidine: (a) 1/0.8 (b) 1/1, and (c) 1.2/1.



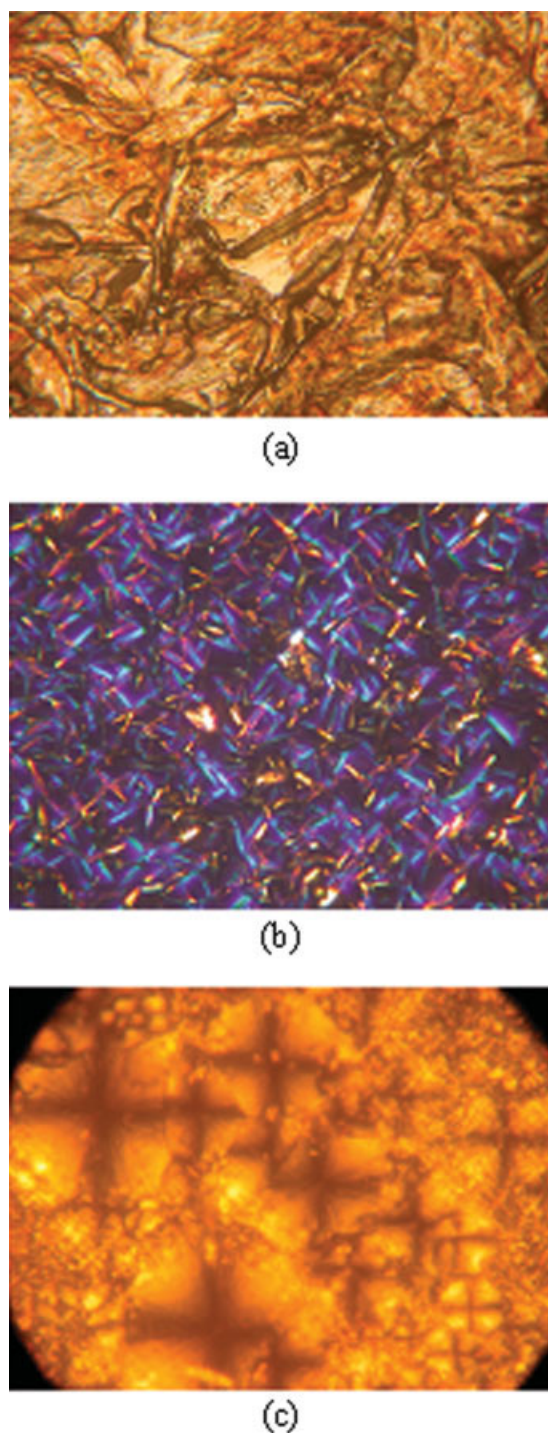


**Figure 4** POM images of *p*-toluidine and PTF with different molar ratios of formaldehyde to *p*-toluidine (magnification = 200 $\times$ ): (a) 0/1, (b) 1/1, and (c) 1.2/1. [Color figure can be viewed in the online issue, which is available at [www.interscience.wiley.com](http://www.interscience.wiley.com).]

and form a smaller structure that contributes to the high-angle diffraction peaks for PTF prepared with excess formaldehyde (formaldehyde/*p*-toluidine = 1.2/1 mol/mol), and the small-size crystal has a spherulitic structure, which is discussed in the following discussion about POM.

## POM

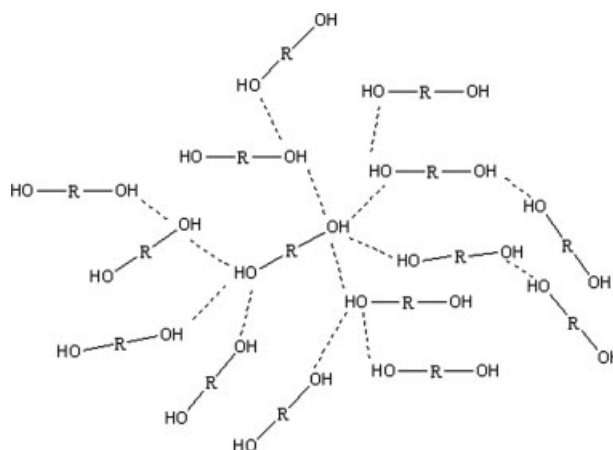
Figure 4 presents POM images of PTF resins with different reaction times and monomer ratios. The brown color of the crystalline structure of the pure *p*-toluidine monomer [Fig. 4(a)] can be clearly identified with POM, and it provides a reference for checking the crystalline structures of PTF prepared under various polymerization conditions. When the monomer ratio for the two monomers is 1, it exhibits a needlelike structure [Fig. 4(b)], which contributes to the X-ray diffraction pattern of Figure 3(a). However, when excess formaldehyde is present during the polymerization, the needlelike structure is destroyed because of the formation of strong hydrogen bonds between the chain ends, and a spherulite-like Maltese cross structure is displayed [Fig. 4(c) and Scheme 2].

## Intrinsic viscosity

Table II presents the intrinsic viscosity, which is related to the molecular weight, of the PTF resin prepared with polymerization times of 24 and 6 h. The measurement was carried out with PTF dissolved in concentrated sulfuric acid solutions. It indicates that a longer polymerization time results in a higher intrinsic viscosity and a higher molecular weight.

## Proton conductivity

Figure 5 presents typical Cole–Cole plots, and the extrapolated bulk resistance of the PTF prepared under various polymerization conditions is listed in Table II. According to the Cole–Cole plots obtained at 100 $^{\circ}$ C for all samples, PTF polymerized for 6 and 24 h showed extrapolated bulk resistance of 214 and 365  $\Omega$ , respectively, at about 30% humidity. The pro-



**Scheme 2** Possible spherulitic structure nucleated and grown by chain-end hydrogen bonding between diol-like PTF molecules.

**TABLE II**  
**Proton Conductivity ( $\sigma$ ) and Intrinsic Viscosity ( $[\eta]$ ) of PTF and Nafion Measured at RT (25°C, 30% RH) and 90–100°C (0% RH)**

PEM	$[\eta]$ (dL/g)	$\sigma \times 10^3$ (S/cm)	
		RT	90–100°C
Nafion		3	0.0125
PTF (1 : 0.8) for 6 h	0.0471	0.142	0.139
PTF (1 : 0.8) for 24 h	0.0667	0.139	0.135
PTF (1 : 1) for 24 h	—	0.147	0.138
PTF with excess CH <sub>2</sub> O for 24 h	—	0.176	0.136
PTF with excess CH <sub>2</sub> O and sulfuric acid for 24 h	—	2.11	3.62
PU prepolymer blended with 70% PTF	—	6.5	—
PU prepolymer blended with 60% PTF	—	3.0	—
PU prepolymer blended with 50% PTF	—	1.54	—

ton conductivity of PTF was determined with eq. (2) and turned out to be  $1.42 \times 10^{-4}$  and  $1.39 \times 10^{-4}$  S/cm, respectively. This illustrates that the proton conductivity of a PTF sample is dependent on the polymerization time, which can control the molecular weight of the resultant polymers. Obviously, the polymer with the larger molecular weight demonstrates poorer proton conductivity because of its higher  $T_g$ , which can deter the movement of the transporting protons. The proton conductivity of PTF prepared with different monomer ratios (formaldehyde/*p*-toluidine) was found to be  $1.39 \times 10^{-4}$ ,  $1.47 \times 10^{-4}$ , and  $1.76 \times 10^{-4}$  S/cm, respectively, at RT, as shown in Table II. This demonstrates that the presence of excess formaldehyde can create more etheryl linkages along the backbones to effectively soften the PTF backbone for higher proton conductivity. However, the proton conductivity in the  $10^{-4}$  S/cm range is not high enough to obtain a fuel cell because even when the thickness is thinned to 25  $\mu\text{m}$  to reduce resistance loss, a conductivity of  $10^{-4}$  S/cm can be converted into 25  $\Omega \text{ cm}^2$ , and for either hydrogen or methanol single fuel cells, the open circuit voltage (maximum voltage) is just around 1.2 V, and

the maximum current is still lower than 0.05 A/cm<sup>2</sup> without consideration of other sources of polarization losses. The low proton conductivity may come from two main factors. One is the lack of effective transporting channels for protons due to the dense/crystalline structure of PTF, and the other originates from the low numbers of proton-transporting media such as sulfonic groups. To achieve higher numbers of proton-transporting media, more sulfuric acid can be added at the later stage of high-temperature refluxing during polymerization, which can lead to a sulfonation reaction, create sulfonic groups for the benzene rings, and increase the proton conductivity to more than 1 order of  $2.11 \times 10^{-3}$  S/cm, as listed in Table II. To create conducting channels for protons, PU has been mixed with PTF. Interestingly, even though PU is not capable of conducting any protons, the proton conductivity only slightly decrease and remains almost the same as that of the pure PTF according to Table II when an equal weight percentage of PU or less is present with PTF. It is believed that introducing PU can separate the ordered PTF structure and create effective channels, allowing the protons to go through the PU

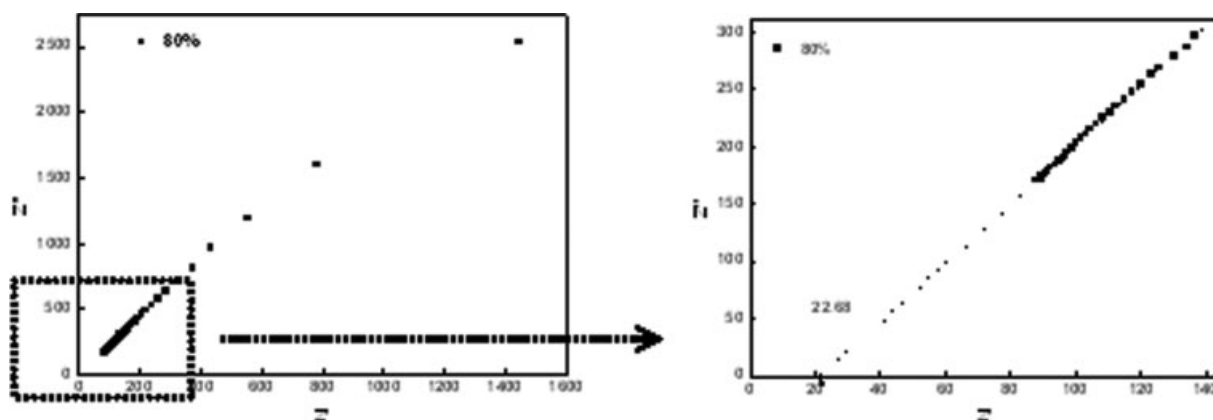


**Figure 5** Typical Cole–Cole diagram of PTF.

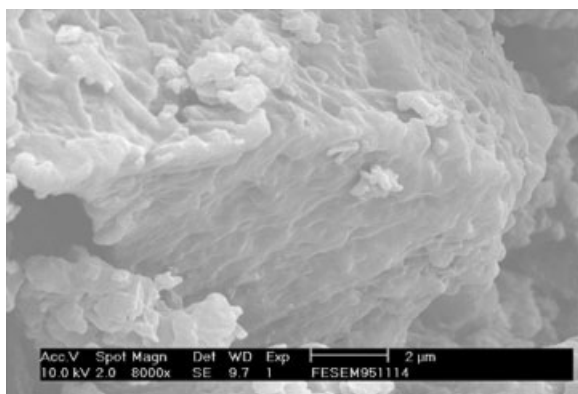


**Figure 6** Scanning electronic microscopy picture of the cross-sectional area of 50% PTF mixed with the PU prepolymer.

matrix because of the incompatibility between PTF and PU, as shown in Figure 6. Besides, the presence of PU can improve the mechanical and methanol-barrier properties of the final blended membrane and keep the proton conductivity.

For comparison with a commercial PEM, Table II also shows the proton conductivity for Nafion, which decreases rapidly from RT ( $3 \times 10^{-3}$ ) to  $100^\circ\text{C}$  ( $1.25 \times 10^{-5}$  S/cm) because of the depletion and evaporation of absorbed water molecules, which are the main conveying media for the protons for a Nafion membrane. However, the proton conductivity of the PTF series shows no significant dependence on the temperature from RT to  $100^\circ\text{C}$ , and this allows the adoption of non-water-containing pure methanol as the fuel source to maximize the output power for a PTF-made membrane electrode assembly (MEA); moreover, the MEA can be operated under a dry condition that always occurs at a high temperature when most of the water product has been evaporated. Therefore, although the proton conductivity of some PTF series listed in Table II is not as high as that of Nafion at RT, the output power of the resultant MEA could be higher than that of the Nafion MEA because the input methanol concentration of the PTF MEA can be elevated to even 100% because of its insolubility and nonwetting property in methanol, which can significantly increase the output current or voltage, which is much higher than that of a regular Nafion MEA. In other words, without consideration of the polarization losses, the proton conductivity of  $10^{-4}$  S/cm from RT to  $100^\circ\text{C}$  is equivalent to  $10^{-2}$  S/cm if pure methanol is used instead of the 1–3% methanol aqueous solution used for a regular Nafion MEA because of its poor methanol-barrier property and strong humidity-dependent proton conductivity, which needs a continuous supply of water from the input aqueous fuel on account of the significant hu-

midity loss at the high-performance temperature (which could reach  $85^\circ\text{C}$ ) of regular fuel cells. Besides, some of the blended films have proton conductivity of the order of  $10^{-3}$  S/cm, which would definitely produce a higher current density for a direct methanol fuel cell whether it is operated at high or low humidities and temperatures.

## CONCLUSIONS

The synthesis of a PTF resin by condensation polymerization in the presence of sulfuric acid has been described, and the effects of the molar ratio of the individual monomers (*p*-toluidine and formaldehyde) and condensation polymerization conditions on the structure of the PTF resin have been studied.

Spectral studies on characterization by FTIR and  $^{13}\text{C}$ -NMR have been performed and prove the presence of the PTF resin. WAXD and POM have been used to examine the effects of the molar ratio and reaction time on the crystallinity and crystalline structure of PTF. It has also been found that PTF can proceed to crystallization because of the absence of isomers in the ortho–para positional polymerization of *p*-toluidine instead of aniline monomer, which always gives the aniline formaldehyde resin, which is not crystallizable at all. A PTF resin with a high molecular weight has poorer proton mobility because of its stiffer structure.

Nafion shows lower proton conductivity than all PTF membranes at temperatures higher than  $90^\circ\text{C}$ , but the PTF series maintains its proton conductivity from RT to at least  $100^\circ\text{C}$  with an insignificant dependence on humidity; this allows the use of non-water-containing pure methanol as a fuel source. PTF molecules can become softer and proton conductivity can be improved by introduction into the backbones with a soft etheryl group from the condensation of the chain-end methanol groups of PTF prepared with excessive formaldehyde.

The low proton conductivity of  $10^{-4}$  S/cm of the PTF series can be improved by sulfonation with sulfuric acid to  $10^{-3}$  S/cm, which can be maintained after blending with PU, which can create open proton conducting channels for pure PTF

Because pure methanol can be used as a fuel source on account of the insolubility and nonwetting property of PTF in it, the output current density is able to be significantly increased if a PTF MEA is assembled.

Future work will cover the copolymerization of PTF diol with PU prepolymer to effectively destroy the ordered structure of PTF for a higher proton conductivity and good mechanical and methanol-barrier properties.

## References

1. Kordesch, K.; Simader, G. *Fuel Cells and Their Applications*; VCH: Weinheim, 1996.
2. Cleghorn, C.; Ren, X.; Springer, T. E.; Wilson, M. S.; Zawodzinski, C.; Zawodzinski, T. A.; Gottesfeld, S. *Int J Hydrogen Energy* 1997, 22, 1137.
3. Ren, X.; Zelency, P.; Thomas, S.; Davey, J.; Gottesfeld, S. *J Power Sources* 2000, 86, 111.
4. Hietala, S.; Maunu, S. L.; Sundholm, F. *J Polym Sci* 1999, 38, 1741.
5. Alberti, G.; Casciola, M.; Massinelli, L.; Bauer, B. *J Membr Sci* 2001, 185, 73.
6. Zaidi, S. M.; Mikhailenko, S. D.; Robertson, G. P.; Guiver, M. D.; Kaliaguine, S. *J Membr Sci* 2000, 173, 17.
7. Mikhailenko, S. D.; Zaidi, S. M.; Kaliaguine, S. *Catal Today* 2001, 67, 225.
8. Smitha, B.; Sridhar, S.; Khan, A. A. *J Membr Sci* 2003, 225, 63.
9. Mohr, R.; Kudela, V.; Schauer, J.; Richau, K. *Desalination* 2002, 147, 191.
10. Staiti, P. *Mater Lett* 2001, 47, 241.
11. Jones, D. J.; Roziere, J. *J Membr Sci* 2001, 85, 41.
12. Weng, D.; Wainright, J. S.; Landau, U.; Savinell, R. F. *J Electrochem Soc* 1996, 143, 1260.
13. Li, Q.; He, R.; Jensen, J. O.; Bjerrum, N. J. *Fuel Cells* 2004, 4, 147.
14. Elabd, Y. A.; Napadensky, E.; Sloan, J. M.; Crawford, D. M.; Walker, C. W. *J Membr Sci* 2003, 217, 227.
15. Murata, K.; Izuchi, S.; Yoshihisa, Y. *Electrochim Acta* 2000, 45, 1501.
16. Wright, P. V. *Electrochim Acta* 1998, 43, 1137.
17. Wen, T. C.; Wang, Y. J.; Cheng, T. T.; Yang, C. H. *Polymer* 1999, 40, 3979.
18. Fenton, D. E.; Parke, J. M.; Wright, P. V. *Polymer* 1973, 14, 589.
19. Wright, P. V. *J Br Polym* 1975, 7, 319.
20. (a) Armand, M. B.; Chabagno, J. M.; Duclot, M. J. In *Fast Ion Transport in Solids*; Vashista, P.; Mundy, J. N.; Shenoy, G. K., Eds.; Elsevier: New York, 1979; p 131; (b) Hardy, L. C.; Shriver, D. F. *J Am Chem Soc* 1985, 107, 3823.
21. Moore, J. A. *Macromolecular Syntheses*; Wiley: Chichester, England, 2000; p 215.
22. Ho, K. S.; Hsieh, T. H.; Kuo, C. W.; Lee, S. W.; Lin, J. J.; Huang, Y. J. *J Polym Sci Part A: Polym Chem* 2005, 43, 3116.
23. Ho, K. S.; Hsieh, T. H.; Kuo, C. W.; Lee, S. W.; Huang, Y. J.; Chuang, C. N. *J Appl Polym Sci* 2007, 103, 2120.
24. Huang, Y. J.; Hsieh, T. H.; Wang, Y. Z.; Chuang, C. N.; Chen, Y. P.; Huang, P. T.; Ho, K. S. *J Appl Polym Sci* 2007, 104, 773.